

# Myosin Head Interactions in $\text{Ca}^{2+}$ -Activated Skinned Rabbit Skeletal Muscle Fibers<sup>1</sup>

Gregory J. Wilson,<sup>\*2</sup> Sarah E. Shull,<sup>†</sup> Nariman I. Naber,<sup>†</sup> and Roger Cooke<sup>†</sup>

<sup>\*</sup>Department of Pathology, D06, The University of Sydney, New South Wales, 2006, Australia; and <sup>†</sup>Cardiovascular Research Institute, and Department of Biochemistry & Biophysics, University of California San Francisco, San Francisco, CA, 94143-0524, USA

Received for publication, March 18, 1997

Interactions between the two myosin heads were studied in skinned rabbit slow-twitch muscle fibers activated in the presence of vanadate ( $\text{V}_i$ ), a phosphate analog. The strong complex between  $\text{V}_i$ , MgADP, and myosin trapped the myosin in an inactivated myosin·MgADP· $\text{V}_i$  state. Electron paramagnetic resonance spectroscopy was used to quantitate the fraction of myosin heads trapped in the presence of a spin labeled analog of ATP (SLATP). Force was found to depend directly on the fraction of untrapped heads. At high [ $\text{V}_i$ ] (low force), most untrapped heads would have a trapped partner. The equivalence of force with the proportion of untrapped heads shows that the isometric force produced by a single untrapped myosin head on a molecule with a trapped partner is equivalent to that produced by either head of a myosin molecule with neither head trapped. The actin-activated MgATPase activities of one-headed and two-headed skeletal myosin species were inhibited similarly by  $\text{V}_i$ , suggesting that trapping one head did not preclude trapping its partner. These data indicate that the two skeletal muscle myosin heads can function without interacting during maximal  $\text{Ca}^{2+}$ -activated force generation.

**Key words:** electron paramagnetic resonance spectroscopy, muscle, myosin, nucleotide analog, vanadate.

The myosin molecule is comprised of a coiled-coil tail from which protrude two globular heads (1). In spite of considerable effort in several laboratories, the reason why vertebrate skeletal muscle myosin has two heads and whether the heads interact during contraction remain unclear (2-6). Cooperativity has been observed between the heads of myosin from animals which use thick filament  $\text{Ca}^{2+}$ -regulation (7), and both heads are necessary for phosphorylation-dependent regulation of smooth muscle myosin (8). However, a number of observations have proven that cooperative interactions between the two heads of vertebrate skeletal muscle myosin are not necessary for it to retain enzymatic and mechanical functions. For example, single-headed myosin and single myosin heads (myosin subfragment 1) can hydrolyze MgATP (9-11), move actin filaments (12, 13), and generate force (14-16).

Although most observations have suggested that cooperative interactions are not necessary for force generation, some results have suggested that such interactions between the heads of mammalian skeletal muscle myosin can occur.

Therefore, this aspect of contraction remains controversial. It is important to use muscle fibers to try to characterize these possible interactions because the myofilament arrays are still intact. In a study using this preparation, it has been suggested that the myosin heads in skinned mammalian skeletal muscle fibers cannot function independently and that blocking the function of one head of a myosin molecule totally inhibits force production by the other head (5). From protein studies, it has also been found that the presence of nucleotides or divalent cations can modify the two heads of a single myosin molecule differently, suggesting that the binding of nucleotide,  $\text{Ca}^{2+}$ , or  $\text{Mg}^{2+}$  to one head modifies the properties of the other head (4, 17).

Therefore, the possibility exists that subtle interactions might occur which modulate myosin function in intact myofilament arrays. A number of possible relationships could exist between the myosin heads. One possibility for interaction could arise if only one head of the pair could generate force at a time. This could happen if for example there were steric constraints placed upon the second head from interacting with the thin filament at the same time as its partner. For this case trapping of one head in a non-force generating state would inhibit force by less than 50%, since the remaining head could take up the slack by cycling more rapidly. Other possible relationships between the heads could include cooperative enhancement or inhibition of function to varying degrees, or independent functioning by the two heads with no interactions. Solving the nature of these interactions will have implications for the independent cross-bridge model of force generation (18).

<sup>1</sup> This work was supported by USPHS grant AR42895, by a Neuromuscular Disease Research Fellowship to GJW from the Muscular Dystrophy Association of America, and by a grant-in-aid from the Muscular Dystrophy Association to RC.

<sup>2</sup> To whom correspondence should be addressed at the present address: Cooperative Research Centre for Cardiac Technology, Block 4, Level 3, Royal North Shore Hospital, St Leonards, NSW 2065, Australia. Phone: +61-2-9926 6123, Fax: +61-2-9901 4097, E-mail: gjw@blackburn.med.usyd.edu.au  
Abbreviations: P, inorganic phosphate ion;  $\text{V}_i$ , vanadate ion.

To investigate possible myosin head interactions, we have used vanadate ( $V_i$ ), an analog of inorganic phosphate ( $P_i$ ), to specifically inhibit myosin head function in skinned rabbit skeletal muscle fibers. Myosin heads are trapped by  $V_i$  in the myosin·MgADP· $V_i$  state, analogous to the myosin·MgADP· $P_i$  state (8, 19–21), which cannot hydrolyze MgATP or produce force (19, 22–26). Trapping is stable in myosin in the absence of actin, or in the relaxed state in muscle fibers, with a long half-life (19, 23, 27). It is highly specific for the nucleotide hydrolysis site on myosin and is completely reversible (21, 23, 26), unlike covalent modifiers which can label several sites (5, 28).

The  $Ca^{2+}$ -activated trapping reaction was followed by monitoring isometric force generation in the fibers. It was then important to correlate the proportion of trapped heads with fiber mechanical properties after they had been trapped at various  $V_i$  concentrations. For this reason a spin labeled analog of ATP (SLATP) was used so that myosin heads were trapped in myosin·MgSLADP· $V_i$  complexes which could then be quantitated by electron paramagnetic resonance (EPR) spectroscopy of the fibers (22, 24, 27).

We have found that force production was diminished when fast-twitch fibers were treated with  $V_i$ , and that the decline in force was consistent with a simple binding isotherm (26). This result indicates that the myosin heads were trapped in a non-cooperative manner. Therefore, at very high [ $V_i$ ] most of the myosin molecules would be in a form in which both heads are trapped and most of the remainder would be in the form having one head trapped. The data show that the isometric force produced by one myosin head is unchanged when its partner has trapped a nucleotide and is unable to interact with actin. This indicates that a myosin head does not preclude the function of its partner during maximally  $Ca^{2+}$ -activated isometric contractions.

#### MATERIALS AND METHODS

**Fiber Mechanics**—Muscle fibers were obtained from rabbit soleus (slow-twitch) muscles, and glycerinated to remove the sarcolemma. Fiber force generation was measured as previously described (26, 29) using a sensitive solid state force transducer coupled to a PC (IBM). Initial sarcomere lengths were determined by He-Ne laser diffraction to be between 2.4 and 2.6  $\mu\text{m}$  (26, 30).

**MgATPase Activity**—The MgATPase activities of actin-activated heavy meromyosin (a two-headed species), myosin S1 (a one-headed species) and myosin (a two-headed species) were determined at 23°C in the presence of  $V_i$  using the modified Malachite Green assay for  $P_i$  generation over time (11) as previously described (26). Previously described methods were also used to prepare actin (9), myosin (10), heavy meromyosin (31), and myosin S1 (31, 32).

**Solutions**—The solution composition, pH, and ionic strength for fiber activation were determined from standard binding constants as previously described (25, 26, 29). The solutions used for relaxing (and activating) fibers comprised magnesium acetate (MgAc<sub>2</sub>, 5 mM), ethylene-glycol-bis-( $\beta$ -aminoethyl ether)- $N,N,N',N'$ -tetraacetic acid (EGTA, 1 mM),  $N$ -tris(hydroxymethyl)-2-aminoethanesulphonic acid (TES, pH 7.0, 25°C, 100 mM), ATP (4 mM), and  $K_2HPO_4$  (5 mM). Creatine phosphate (20 mM) and creatine phosphokinase (1 mg/ml) were used to regen-

erate ATP, but were ineffective for regeneration of SLATP from SLADP. KAc was added to bring the ionic strength to 210 mM. To make activating solutions, calcium ions were added to the relaxing solution as a stock solution of  $CaCl_2$  so that the final [free  $Ca^{2+}$ ] of the activating solutions was  $\geq 0.03$  mM (28, 29).

**Vanadate Solutions**—Stock solutions of sodium metavanadate ( $NaVO_3$ ), or of vanadium oxide ( $V_2O_5$ ) of around 100 mM were made as previously described (19, 25, 26). The stock solutions were raised to pH 10 to reduce polymerization and were boiled prior to being used to hydrolyze polymerized species. When  $V_i$  in this stock solution was added to activating solutions containing high [TES] (100 mM) over the range of experimental [ $V_i$ ] used in this study, increases of not more than 0.1 pH unit were observed. Polymerization, indicated by yellow coloration (19), was not observed. When the [ $V_i$ ] in the experimental solutions was as high as 15 mM, corrections were made to the contents of the rigor and ATP solutions to account for changes in ionic strength and solute concentrations.

**Synthesis and Properties of Spin-Labeled ATP**—The electron paramagnetic resonance (EPR) spectra were derived from the TEMPO spin-labeled (SL) analog of ATP [3'-deoxy-2'-(2,2,5,5-tetramethylpyrrolidine-1-oxyl-3-carboxylate) adenosine 5'-triphosphate], which was synthesized as previously described (24). The TEMPO moiety was linked to the ribose ring by an ester bond. A hydrogen atom replaced the hydroxyl group at the 3' position of the ribose ring to prevent isomerization of the TEMPO spin label moiety between the 2' and 3' positions. This SLATP analog binds specifically at the nucleotide binding site of myosin (24).

Slow-twitch fibers were used for EPR experiments. We have found that slow-twitch fibers bind SLATP much tighter than fast-twitch fibers do, with a  $K_{app}$  of  $10^5$  M<sup>-1</sup> for slow-twitch fibers, compared with a  $K_{app}$  of  $10^4$  M<sup>-1</sup> for fast-twitch fibers (24). Another reason for using only slow-twitch fibers is that SLATP is not a good substrate for creatine kinase. Therefore it cannot be regenerated during active contraction. Fast-twitch fibers would use the MgSLATP faster than it could diffuse into the fibers, which would result in a build-up of rigor cross-bridges in the center of the fibers. However, since slow-twitch fibers hydrolyze MgATP (and MgSLATP) more slowly, this is less likely to happen.

This SLATP analog elicits contractile responses of slow-twitch fibers which are similar to results obtained using normal ATP. Therefore the conclusions derived from experiments using this analog can be extrapolated to the physiological properties of the fibers under normal conditions. However, fibers were not relaxed until the [MgSLATP] reached around 400  $\mu\text{M}$ . Therefore at concentrations lower than this the fibers were activated. Maximum  $Ca^{2+}$ -activated tension generation at the saturating concentration of [SLATP] (400  $\mu\text{M}$ ) is  $60 \pm 15\%$  (mean  $\pm$  SE,  $n=5$ ) of that attained using normal ATP at the same temperature, and the velocity of shortening under zero load and the  $Ca^{2+}$ -activated MgATPase activities are around  $30 \pm 10\%$  (mean  $\pm$  SE,  $n=5$ ) of the maximum. SLATP has a  $K_{diss}$  for binding to the active site during maximal  $Ca^{2+}$ -activation of around 17  $\mu\text{M}$  in slow-twitch fibers.

**Determination of Fiber Myosin and MgSLADP· $V_i$  Contents**—The fiber bundles were removed from the flow

cell for determination of myosin content and  $V_i$ -trapped MgSLADP content. After washing extensively in a relaxing solution containing MgATP (4 mM), the fibers were sonicated in 50  $\mu$ l of either guanidine-HCl (6 M) and MgATP (1 mM), or in KCl (0.6 M), MgATP (1 mM), and urea (6 M), to denature the heads and thereby liberate all of the trapped SLADP. The amount of SLADP released was determined by EPR spectroscopy. This was compared with the amount of myosin present in the bundles, determined using Coomassie Brilliant Blue G. It was assumed that myosin comprised 45% of the total protein content of the fibers (14). The number of trapped heads was then compared with the EPR spectra obtained for the same sonicated fiber bundles after activation in the presence of  $V_i$ . These values were then compared with the level of force decline for fibers on the tensiometer maximally  $Ca^{2+}$ -activated in the presence of MgSLATP at the same  $[V_i]$ .

**Recording Electron Paramagnetic Resonance (EPR) Spectra**—The techniques used to collect EPR spectra were similar to those described previously (24, 33). First derivative X-band microwave absorption spectra were recorded using an ER/200D EPR spectrometer (IBM Instruments, CT, USA). The following instrument settings were used: microwave power 27 mW; modulation 0.2 millitesla at 100 kHz. Fiber experiments were performed using a flow cell in a TE<sub>110</sub> cavity. The cell comprised a narrow (0.7 mm internal diameter) capillary in which the fibers (~50) were isometrically suspended using surgical silk (Deknatel No. 10). The capillary was aligned parallel with the static magnetic field ( $H_0$ ) and solutions could be passed into and out of this capillary through the top of the cell. The EPR spectrometer was interfaced to a PC (IBM) with an analog/digital board. Spectra were collected at 22–24°C and averaged on the PC (IBM) using software written in PC/FORTH (Version 3.2, Laboratory Microsystems, CA, USA).

The fraction of active myosin heads was calculated from EPR spectra (see Figs. 3 and 4). The fraction of active heads (1 minus the proportion of disordered heads) was the difference between the total number of labeled heads (calculated from peaks 2 and 3, Fig. 3) and the proportion of disordered (trapped) heads (calculated from peak 3, Fig. 3). Any peak height of the down-field peak (peak 3) representing trapped heads in the EPR spectrum of this spin probe represents twice the number of spin labels as an equivalent peak height of the more up-field peak (peak 2) representing ordered heads (24).

## RESULTS

**Effects of Vanadate upon Maximally  $Ca^{2+}$ -Activated Force**— $V_i$  inhibited the ability of skinned rabbit slow-twitch muscle fibers to generate force in the presence of both MgATP and MgSLATP. Figure 1 shows a typical trace obtained for a fiber activated in the presence of MgSLATP. The fiber was first immersed in a rigor solution. When SLATP (200  $\mu$ M) was added to the fiber well, force was initially generated rapidly. At this [SLATP] the fibers did not relax (see "MATERIALS AND METHODS"). Force-velocity data were collected under these circumstances, showing that the fiber could contract with a maximum contraction velocity of  $30 \pm 10\%$  (mean  $\pm$  SE,  $n=12$ ) of that found for MgATP. This suggests that the fiber was generating active

force rather than generating rigor force. When  $Ca^{2+}$  ions were added, no substantial increase in force generation was detected other than the slow increase observed prior to the addition of  $Ca^{2+}$ . Similar forces were obtained when  $V_i$  was added at low concentrations (2  $\mu$ M), indicating that this concentration was too low to appreciably inhibit force. However, when  $V_i$  was added at a high concentration (16 mM), force declined rapidly as the myosin heads in the fibers were trapped by  $V_i$ , reaching a steady state in this case at around 28% of maximal force. The time to half force inhibition ( $t_{1/2}$ ) was 5 s, as was found for fast-twitch fibers activated in the presence of MgATP and trapped at high  $[V_i]$  (26). We also found that the  $t_{1/2}$  for force inhibition in slow-twitch fibers activated in the presence of MgATP was around 5 s at the  $[V_i]$  where force was reduced to less than 30%. Thus the kinetics of  $V_i$  binding to the myosin heads also suggested that the fiber myosin heads were cycling actively in the presence of MgSLATP.

EPR experiments were performed on bundles of fibers that were secured inside a capillary and perfused rapidly by a solution flowing through the capillary, with a flow rate of approximately 2 cm/s. In contrast, the forces shown in Fig. 1 were produced by a single fiber activated in the well of the tensiometer. The rapid flow in the capillary was thought to force the solution through the bundles, producing perfusion that was similar to that observed for the single fibers. To test this hypothesis we measured the force and the MgATPase rate for bundles of fibers in the capillary. Fiber bundles were mounted as for the EPR experiments and perfused with a solution as described in Fig. 1. One end of the capillary was open and the thread securing the fiber bundles was connected to a glass rod that was fixed to a solid state force transducer, allowing the tension of the bundle to be measured. In the presence of 200  $\mu$ M MgATP the bundles generated a large  $Ca^{2+}$ -activated tension,  $300 \pm 75$  kN/m<sup>2</sup> (mean  $\pm$  SE,  $n=5$ ). The  $Ca^{2+}$ -activated tension

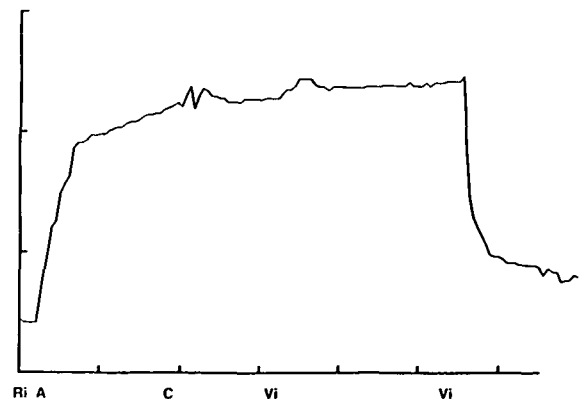


Fig. 1. Trace showing a typical protocol for  $Ca^{2+}$ -activating skinned rabbit slow-twitch muscle fibers in the presence of MgSLATP and then trapping myosin heads with  $V_i$  and MgSLADP. The fiber was first kept in a rigor solution ( $R_i$ ) with the length adjusted so that the fiber was just taut. It was then activated by the addition of MgSLATP (200  $\mu$ M) in the absence of  $Ca^{2+}$  (A). To ensure that the fiber was fully activated,  $Ca^{2+}$  ions ( $[Ca^{2+}] \geq 0.03$  mM) were then added (C).  $V_i$  was then added at two concentrations ( $V_i$ ), first at 2  $\mu$ M and then at 16 mM, until steady state force was reached. The temperature was 25°C. The ticks on the horizontal axis represent 1 min each and those on the vertical axis represent 200 kN/m<sup>2</sup> of force.

generated in the presence of 200  $\mu\text{M}$  MgSLATP was approximately  $140 \pm 45 \text{ kN/m}^2$  (mean  $\pm$  SE,  $n=5$ ), *i.e.*, close to 50% of that generated in the presence of MgATP. The force rose to a maximum in 30 s, which is only a little slower than for a single fiber, and addition of 16 M  $V_i$  decreased the force to 10% of the control level in 20 s. These rates of force change are only a little slower than for a single fiber, showing that perfusion of the fibers in the EPR cell is rapid. The hydrolysis rate of the MgSLATP by bundles of soleus fibers was measured by collecting the solution that had passed through the capillary and determining the concentration of  $P_i$ . The hydrolysis rate was found to be  $0.2 \pm 0.05 \text{ s}^{-1}$  per myosin head (mean  $\pm$  SE,  $n=5$ ) at  $20^\circ\text{C}$ , which was close to the value of  $0.3 \pm 0.05 \text{ s}^{-1}$  per myosin head (mean  $\pm$  SE,  $n=5$ ) at  $20^\circ\text{C}$  measured for single fibers in solution in the presence of MgSLATP, where perfusion was less of a problem. Together these results suggest that the myosin heads were cycling in the fibers in the EPR cell in a fashion that was similar to those in single fibers for which the mechanics were measured. Although some rigor core in the fibers in the EPR cell cannot be excluded, the results suggest that most of the heads are actively cycling. The problem of the rigor core will be diminished at higher concentrations of  $V_i$ , where the hydrolysis rate of the fibers is also diminished, as outlined in the "DISCUSSION." These results also suggest that the fibers were able to maintain large forces for extended periods, without loss of  $\text{Ca}^{2+}$ -activated MgATPase activity. This suggests that the fibers were in good condition throughout these experiments.

Force generation was inhibited by  $V_i$  in a concentration-dependent manner, as was found previously for fast-twitch fibers (23, 25, 26). Figure 2 shows that there were differences in the effects of  $V_i$  upon isometric force generation in slow-twitch fibers activated in the presence of either MgATP or MgSLATP.

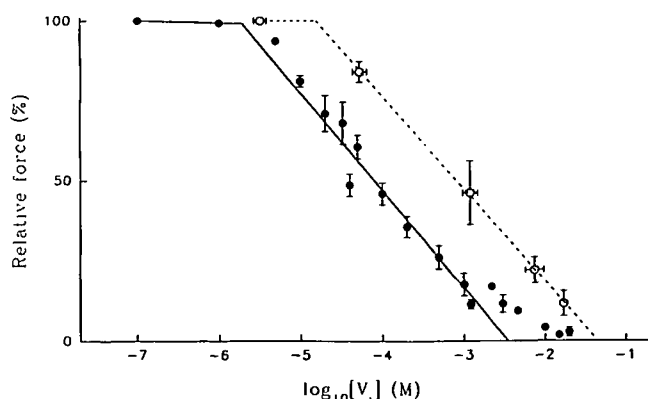


Fig. 2. Relative maximally  $\text{Ca}^{2+}$ -activated isometric force *vs.*  $\log_{10}[V_i]$  for slow-twitch skinned rabbit skeletal muscle fibers in the presence of  $P_i$  (5 mM) and either MgATP ( $\bullet$ , 4 mM) or MgSLATP ( $\circ$ , 200  $\mu\text{M}$ ). Relative force was determined at  $25^\circ\text{C}$  by comparing the force obtained during  $\text{Ca}^{2+}$ -activation in the presence of  $V_i$  to that obtained either before or after this when the fiber was activated in the absence of  $V_i$ . The bars represent the standard error about the mean [ $3 \leq n \leq 8$  fibers for each data point, and in some cases each fiber was activated in the presence of more than one  $[V_i]$  (see Fig. 1)]. Curves were fitted by linear regression to the points for  $[V_i]$  between 3  $\mu\text{M}$  and 1.2 mM for MgATP ( $r^2=0.96$ ) and between 53  $\mu\text{M}$  and 17 mM for MgSLATP ( $r^2=0.98$ ).

**ATP**—The inhibition by  $V_i$  of force generation in slow twitch fibers in the presence of MgATP (4 mM) was examined using a similar protocol to that shown in Fig. 1 of Wilson *et al.* (26). The maximally  $\text{Ca}^{2+}$ -activated force generated by slow-twitch fibers in the presence of MgATP remained fairly high until the  $[V_i]$  reached about 3  $\mu\text{M}$ . As the  $[V_i]$  increased above this level, maximally  $\text{Ca}^{2+}$ -activated isometric force declined fairly linearly in proportion to the  $\log_{10}[V_i]$ . A line of best fit was therefore calculated from values obtained between  $[V_i]$  of 3  $\mu\text{M}$  and 1.2 mM. At around 1.2 mM  $V_i$ , the decline in force began to level out and at 3 mM  $V_i$ , the force had declined to around 10%.

**Spin-Labeled ATP**—In the presence of MgSLATP the curve fitted to the force decline as  $[V_i]$  increased was similar in shape to that obtained using MgATP. Thus the range of  $[V_i]$  required to titrate the force from its maximal level to zero was the same for MgATP and MgSLATP in slow twitch fibers. However, while the  $[V_i]$  at which force generation was reduced to half was 90  $\mu\text{M}$  using MgATP, it was around 1.1 mM for MgSLATP. Thus the fibers were approximately 12 times less sensitive to  $V_i$  when activated in the presence of MgSLATP, and the curve was shifted significantly to the right. The linear regression curves were significantly different from each other at the 99% confidence level when individual data points were analyzed.

This difference in inhibitory characteristics reflects differences in the structure of the SLATP analog. It shows that the effective binding constant of  $V_i$  has been altered by the spin label moiety attached to the ribose ring of ATP (see "MATERIALS AND METHODS"). Covalent modifications to the ribose ring have previously been found to affect binding to the myosin active site, the magnitude of the effect depending upon the specific modification. However, although the effects were significant, they were not debilitating in this study.

**EPR Spectra of  $\text{Ca}^{2+}$ -Activated Fibers**—To determine the relation between force and the trapping reaction, the proportion of trapped myosin heads was determined from the electron paramagnetic resonance (EPR) spectra of spin-labeled ADP (SLADP) trapped on the heads of slow-twitch fibers using  $V_i$ . The experiments were performed with the fibers isometrically suspended within a flow cell in the  $\text{TE}_{110}$  cavity of the EPR spectrometer (24, 33). This allowed solutions containing SLATP,  $V_i$  at various concentrations,  $\text{Ca}^{2+}$  and other solutes to be passed around the fibers under pressure. The turbulent flow generated aided the perfusion of the fiber bundles. This led to the trapping of myosin in the myosin-MgSLADP- $V_i$  complex during  $\text{Ca}^{2+}$ -activation in a  $[V_i]$ -dependent manner, which was analogous to the trapping reaction which occurred during activation using normal MgATP (24-26). Only the down-field portions of the EPR spectra are shown, since they illustrated the pertinent data with better resolution than did spectra recorded using a wider sweep (Figs. 3 and 4). The large, up-field peaks indicate spin-labeled nucleotide not bound to myosin (Peak 1). The other two peaks represent spin-labeled nucleotide which was bound to the myosin heads.

The experimental protocol was as follows. Bundles of slow-twitch fibers ( $\sim 50$ ) were first mounted in the flow cell and an EPR spectrum was obtained with the fibers  $\text{Ca}^{2+}$ -activated in the presence of SLATP and in the absence of

$V_i$ . Most of the bound probes in this situation were ordered (Fig. 3). We then maximally  $Ca^{2+}$ -activated the fibers in the presence of MgSLATP at various  $[V_i]$  until the spectra had reached their steady states at each  $[V_i]$ .

In the absence of  $V_i$ , the more up-field of the bound EPR peaks (Peak 2), representing the ordered spin probe, is the predominant of the bound peaks, with a small disordered peak representing about 10% of the probes. The second peak represents myosin heads that are detached from actin in the cycle. The fraction of ordered probes is greater than seen for probes attached to Cys-707 (34). This shows that the presence of the spin probe alters the myosin cycle, so that a greater fraction of myosin heads are bound to actin. The ordered peak diminished when  $V_i$  was added to the perfusing solution and continued to diminish as the  $[V_i]$  increased. Concomitantly the down-field disordered peak (Peak 3) became larger. Peak 2 represents the amount of spin-labeled nucleotide bound to force-producing cross-bridges and not yet trapped by  $V_i$ , while peak 3 arises from labeled nucleotides (SLADP) trapped on the myosin heads by  $V_i$ . The intensities of both of these peaks were measured to determine the exact ratio of ordered to disordered heads at different  $[V_i]$ . The amplitude of a unit peak height of a disordered peak (Peak 3) represents twice the number of spin labels as an equivalent peak height of an ordered peak (Peak 2) (24).

**Stoichiometry of Trapped SLADP**—We addressed the possibility that SLADP was being trapped on only a fraction of the myosin heads. In particular, this would occur if the trapping of one head prevented its partner from also being trapped, or if not all of the heads are simultaneously recruited during maximal  $Ca^{2+}$ -activated force generation. It was therefore necessary to determine the proportion of heads trapped at high levels of  $V_i$ . To measure this, the

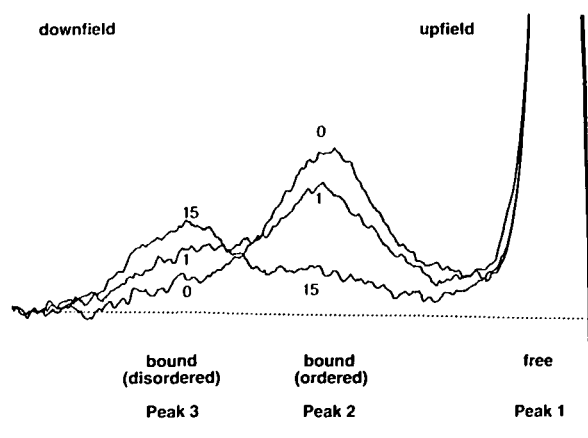


Fig. 3. Superimposed EPR spectra of spin-labeled nucleotides on the myosin heads of a bundle of isometrically  $Ca^{2+}$ -activated rabbit slow-twitch fibers in a flow cell at 22–24°C. The numbers beside the spectra indicate increasing  $[V_i]$  in mM. Spectra were taken with a 20 Gauss sweep and a 3,465 Gauss center field. Gain and modulation were the same in each case. The free peaks represent MgSLATP in the activating solution not bound to myosin (Peak 1). The bound and ordered peaks represent spin-labeled nucleotide on contracting heads which were not yet trapped with  $V_i$  (Peak 2). The bound and disordered peaks represent cross-bridges trapped by  $V_i$  in the myosin·MgSLADP· $V_i$  state which produces no force (Peak 3). The broken line represents the baseline from which measurements were taken.

fibers were  $Ca^{2+}$ -activated in the presence of MgSLATP and high  $[V_i]$ . The free SLATP was then washed out of the fiber bundles using MgATP, leaving only SLADP trapped by  $V_i$ . To confirm this process the reaction was performed in the flow cell inside the EPR spectrometer, since bound and free spin labeled nucleotide could be distinguished, as shown in Fig. 3.

To determine the stoichiometry of  $V_i$ -trapped SLADP, bundles of slow-twitch fibers were first  $Ca^{2+}$ -activated in the presence of  $V_i$  (15 mM) and MgSLATP (200  $\mu$ M) and then relaxed by several washes using relaxing solutions containing MgATP (4 mM) with negligible free  $Ca^{2+}$ . Superimposed EPR spectra for an activated and washed fiber bundle are shown in Fig. 4. The up-field peak (Peak 1), representing free (unbound) SLATP, became markedly reduced after washing with MgATP. An ordered peak representing contracting heads (Peak 2) is visible for the activated fibers since at this  $[V_i]$  force is not abolished during activation in the presence of SLATP (see Figs. 1 and 2). This peak disappears upon relaxation with MgATP, since nucleotide is not trapped on this population of the myosin heads. The disordered peak representing relaxed, trapped heads (Peak 3) is not significantly changed in position or magnitude after relaxation with MgATP, indicating that the myosin·MgSLADP· $V_i$  complex is stable for the duration of both our force and EPR experiments, as was found for insect flight muscle (27). Similarly treated single soleus fibers invariably returned to resting force levels when activated and relaxed repeatedly using this protocol on the tensiometer.

The fibers were removed from the flow cell and sonicated for determination of the total amount of myosin trapped in the myosin·SLADP· $V_i$  state. When fiber bundles were  $Ca^{2+}$ -activated in the presence of 15 mM  $V_i$ , the molar ratio

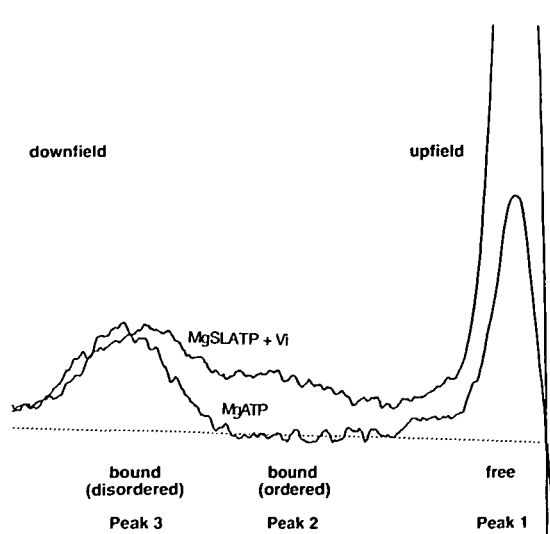


Fig. 4. Superimposed EPR spectra obtained for the same bundle of rabbit slow-twitch fibers in the flow-cell shown in Fig. 3 which were first activated at 22–24°C in the presence of  $V_i$  (15 mM) and MgSLATP (200  $\mu$ M) until the steady state was reached, and then relaxed at 22–24°C for 65 min in the presence of MgATP (4 mM) and the absence of  $V_i$ . The sweep width was 20 Gauss and the center field was 3,450 Gauss. The gain and modulation were the same for each spectrum. The broken line represents the baseline from which measurements were taken.

of SLADP:myosin heads detected using EPR after fiber denaturation was  $78 \pm 7\%$  (mean  $\pm$  range,  $n=2$  bundles) of the amount of myosin heads in the fibers. This is not significantly different from the level of force inhibition obtained at this  $[V_i]$  using single fibers activated in the presence of MgSLATP ( $86 \pm 4\%$  inhibition, mean  $\pm$  SE,  $n=3$ , Fig. 2). This shows that most or all of the myosin heads in mammalian skeletal muscle fibers can bind MgSLADP simultaneously during maximal  $Ca^{2+}$ -activation, including the two heads on the same myosin molecule. If the trapping of one head precluded trapping of its partner, then less than 50% of the heads would be trapped. Therefore, the proportion of heads with bound MgSLADP (both ordered and disordered) in the EPR spectra (Figs. 3 and 4) represented all of the myosin heads in the fibers.

**Relation of Force to Proportion of Active Heads**—The proportion of heads trapped in the myosin·MgSLADP· $V_i$  state was plotted against the  $\log_{10}[V_i]$ . Slow-twitch fiber bundles  $Ca^{2+}$ -activated in the presence of MgSLATP in the flow cell showed that the  $[V_i]$  for achieving half maximal trapping of MgSLADP (1.6 mM) is very close to that for inhibiting force generation in the presence of MgSLATP by half (1.1 mM) (Fig. 5A). To confirm the relationship between the inhibition of force and the proportion of disordered heads, the force was plotted as a function of the fraction of ordered heads (not trapped; Fig. 5B). When fitted by linear regression the data yielded a slope of 0.83 ( $r=0.97$ ) with the intercept at the origin. This line was not significantly different from a slope of one. When the data for force levels below 40% of the maximum were fitted, the slope increased to 0.85 ( $r=0.99$ ). At these high  $[V_i]$ , the lower force levels would be associated with much lower MgSLATPase activities, providing more accurate data (Fig. 6; Ref. 26).

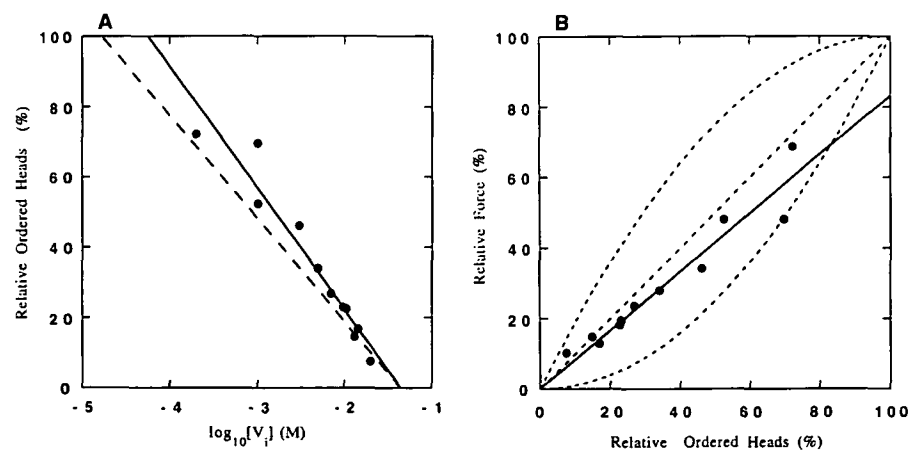
The amount of trapped MgSLADP increased in close proportion to the decrease in force generation as the  $[V_i]$  increased, especially at very high  $[V_i]$ , where the effects of

a possible rigor core in the fiber bundles would have been diminished due to the relatively lower MgSLATPase rates. This shows that the heads were trapped independently and that the proportion of force generation is proportional to the number of free heads. These results support the hypothesis that the two myosin heads can act independently in force generation.

**MgATPase Activity**—The possibility exists that either positively or negatively cooperative  $V_i$ -trapping of the two myosin heads might occur. One of our major hypotheses is that the trapping by  $V_i$  of one head of a myosin molecule does not influence the trapping of the other. We have shown that trapping one head does not prevent its partner from being trapped. However, it was necessary to show that the heads were not trapped simultaneously, which could occur if there was total positive cooperativity between the heads of a myosin molecule, and that there was no negative influence upon trapping the second head by the trapping of the first head.

In order to test the hypothesis that there is no cooperativity in the trapping reaction, we studied the trapping by  $V_i$  during actin-activated MgATPase assays of single-headed myosin subfragment-1 (S1), double-headed heavy meromyosin (HMM) and double-headed myosin from fast skeletal muscle. If the trapping of the two heads was highly positively cooperative, then less  $V_i$  would be required to trap HMM or myosin than S1. A lower  $[V_i]$  would also be needed to inhibit the MgATPase activities of double-headed species if the trapping of one head inhibited the activity of its partner. We found however that the same concentration of  $V_i$  (1.5 mM) was required to inhibit the acto-HMM, actomyosin and acto-S1 MgATPase activities to 50% of maxima (Fig. 6). In fact, the results in Fig. 6 show that the trapping reaction proceeded in an almost identical fashion for the three myosin species. Therefore, the function of one head of the pair does not alter the function of the remaining head. The curves shown in Fig. 6 are steeper

**Fig. 5. Relationship between force generation and trapping of MgSLADP on myosin heads in rabbit slow twitch fibres.** A: Relative proportion of ordered (active) heads vs.  $\log_{10}[V_i]$  for slow-twitch fibers maximally  $Ca^{2+}$ -activated in the presence of MgSLATP (200  $\mu$ M). The data for the proportion of disordered heads were obtained from EPR spectra of fiber bundles activated at 22–24°C in the presence of  $V_i$  in the flow cell (see Fig. 3) as described under "MATERIALS AND METHODS." The solid line is linear regression fitted to data points representing individual measurements to fiber bundles activated at different  $[V_i]$ . The broken line, included for easy comparison, is the regression line from Fig. 2 fitted to the data for force decline in slow-twitch fibers in the presence of MgSLATP and various  $[V_i]$ . B: Relationship between inhibition of force by  $V_i$  and trapping of MgSLADP on myosin heads by  $V_i$  (reduction in proportion of ordered heads). Data were obtained by comparing the proportion of disordered heads with force generation at the same  $[V_i]$ . At points where force and EPR spectra were measured at the same vanadate concentration the force is simply measured directly. At points where EPR data were obtained and force was not measured extrapolation was made between different forces using the solid line in A. The heavy straight line represents a linear fit to the data ( $r^2=0.99$ ). The straight broken line represents the relation expected if force is exactly proportional to the fraction of heads not trapped. The upper and lower broken curves respectively represent the relation expected if a myosin with one head trapped exerts full or zero force relative to that exerted by myosin with neither head trapped. They were generated using a second order polynomial.



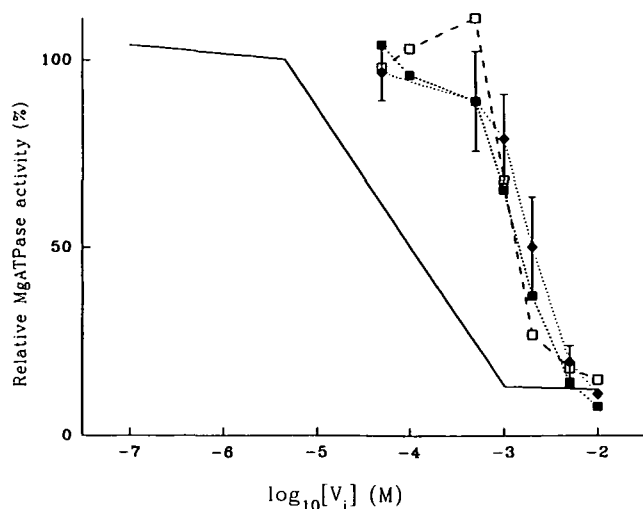


Fig. 6. Effects of  $V_i$  upon relative actin-activated MgATPase activity for rabbit fast skeletal muscle myosin (20  $\mu\text{g/ml}$ , dotted line), myosin S1 (18  $\mu\text{g/ml}$ , long dashes), and heavy meromyosin (20  $\mu\text{g/ml}$ , short dashes). Rabbit skeletal muscle F-actin was used, with G-actin at a 4-fold molar excess as to the myosin species in each case. The solid line represents the effects of  $V_i$  upon relative maximally  $\text{Ca}^{2+}$ -activated MgATPase activity for isometrically contracting rabbit fast-twitch fibers at 25°C (Ref. 26). MgATPase activity was always measured using a Malachite Green method for the determination of  $P_i$  production through the hydrolysis of MgATP at 23°C.

than expected for a simple binding reaction. The reason for this is not clear, although tighter binding of polymeric species of vanadate, which may be present at the higher concentrations of  $V_i$ , may account for some of the steepness.

There is a difference in the inhibition by  $V_i$  of the MgATPase activity of the three myosin species compared with the inhibition of fiber force generation or MgATPase activity (Fig. 6; Ref. 26). Vanadate binds to the actin-myosin-ADP state at the beginning of the power stroke. The population of this state in isometric fibers is much higher because the myosin heads in fibers cannot proceed through the power stroke. In solution, myosin heads in this state go immediately to the end of their power stroke, so that the population of heads in the actin-myosin-ADP state is very small. Because of its shorter lifetime in solution, a higher  $[V_i]$  is required to bind to this state (26).

#### DISCUSSION

**Myosin Head-Head Interactions**—Whether the myosin heads cooperate during their functional interaction with actin has long been a question in the field of contractility. While a number of results exclude the possibility that cooperative interactions between myosin heads are necessary for function, they do not eliminate the possibility of interactions under physiological conditions between the heads which could play a role in modulating contraction. Several results have suggested that binding of one head strongly to actin prevents the second head from binding as strongly (35). In the rigor interaction this is presumably due to the conformational strain that would be required for both heads to make a stereospecific interaction with actin.

Studies using spin-labeled muscle fibers in the presence of pyrophosphate and AMPPNP have shown that one myosin head of a pair could be dissociated more easily than the other and that this did not change fiber stiffness (29, 36, 39). These results suggest the possibility that only one head of a myosin molecule may form a strong force-producing bond with actin at any one time. Thus elimination of the function of one head may allow the other head to work more efficiently by effectively taking up the slack. This possibility is also indicated by studies of fibers modified with spin labels described below.

Some studies have suggested that chemical modification of one of the heads can have a pronounced effect on the function of the remaining head. In one such study myosin heads were modified by cross-linking two reactive sulphhydryls, thus eliminating the ability of the myosin head to interact with actin in skeletal muscle fibers (5). It was concluded that covalent cross-linking of amino acids on one myosin head effectively eliminated the ability of the other head to generate force. Another recent study has suggested that modification of the SH-1 groups on some myosin heads in a fiber alters the ATPase activity of the remaining unmodified heads (37). It is thus possible that the presence of a modified or inactive head influences the action of its neighbor. However, such an interpretation could also arise because the chemical modifications are less specific than thought. A covalent modifier was used to label the myosin heads of skinned fibers (5), which does inhibit myosin head function by affecting the MgATPase properties of the myosin head (38), but which can produce complex effects in the contractile proteins, including complex changes to  $\text{Ca}^{2+}$ -activation properties (28).

Our studies were also motivated by the need to assess the effects of attaching spin labels to myosin heads in fibers. An earlier study found that modification of 50% of the myosin heads with a spin-label attached to the SH1 has very little effect on fiber tension (39). However, SH1 modification is known to modify the actomyosin interaction in solution (28, 38, 40), raising the possibility that the effect of modifying one head was masked because the tension generated by the remaining head was increased. We show below that this possibility is very unlikely.

**Could the  $V_i$ -Trapping Reaction be Cooperative?**—We found that the inhibition of force by  $V_i$  followed the simple binding isotherm expected for the non-cooperative binding of a ligand to a protein (26). This result strongly suggests that the trapping of nucleotides by  $V_i$  is not a cooperative process. However, it does not eliminate several possibilities involving strong cooperativity between the heads. Thus we examined the possibility that trapping of nucleotides by the two heads is highly positively cooperative. If such positive cooperativity existed, the trapping of a myosin-MgADP- $V_i$  complex on one myosin head would greatly facilitate the trapping of a similar complex on the other myosin head. Similarly, if the trapping of one head prevented its partner from being trapped by  $V_i$  but also eliminated its ability to generate tension, this would also suggest a degree of functional dependence between the heads. Both of these possibilities would mean that the trapping of the two heads was not independent.

If trapping of one head of a myosin molecule either prevented or caused the trapping of its partner, then less  $V_i$  would be needed to inhibit double-headed myosin species

with equivalent moles of heads. Our results showed that the relative actin-activated MgATPase activities of both single-headed and double-headed myosin species have a similar dependence upon  $[V_i]$  (Fig. 6). This indicates that the trapping of one head neither prevents nor obliges trapping of its partner on the same myosin molecule. This indicates that the trapping of the two heads is not cooperative, and that it is not necessary for the two heads to function together. This provides further evidence that the heads do not interact during interaction with the thin filament.

*Cooperative Interactions between the Heads of Myosin in Active Fibers*—Some of the observations discussed above raise the possibility that myosin heads may interact in some way during active force generation and shortening. Our study addresses the possibility of cooperative interactions in two ways. First, we have shown that selective removal of the actomyosin interaction by trapping a nucleotide on the cross bridges with  $V_i$  causes a decrease in isometric force that is stoichiometric with the fraction of heads trapped. We have also determined that the heads are trapped independently by  $V_i$  (discussed above). Both of these results suggest that no interactions occur either between the two heads of the same molecule or between heads in adjacent molecules. The data are most definitive at high concentrations of  $V_i$ .

We assumed that the trapping of nucleotides is a random process and calculated the proportion of myosin molecules which will have neither, one or both heads trapped at any particular  $[V_i]$ . These possibilities are plotted in Fig. 5B, along with the data and the linear regression to the data. Most of the data lie close to the line with a unit slope—that is, the relation expected for no cooperative interactions. For instance, at very low levels of force most myosin heads would be trapped and most of the free myosin heads would have a partner which is trapped. At a  $[V_i]$  where 90% of the myosin heads are trapped and 10% are free to cycle ( $p=0.9$ ), one would expect that 81% of the myosin molecules would have both heads inactive, 18% would have one active head, and 1% would have two active heads. Thus if both heads are required for force generation the force expected would be only 1%, and if one-headed myosin generated the same force as two-headed myosin the force would be 19%. Inspection of Fig. 5 shows that both of these possibilities lie outside the experimental error. The observed force at  $p=0.9$  is  $0.08 \pm 0.03$  ( $n=5$ ), which is not significantly different from the value of 10% expected if trapping one head does not affect the tension generated by its partner. That is, the force generated was proportional to the number of untrapped heads. The data lie slightly below a direct proportionality between force and the fraction not trapped, particularly at high forces, although the deviation is not statistically significant. This could be due to a small fraction of SLADP-myosin complexes at low  $[V_i]$ , or could reflect a slight tendency for a trapped head to negatively affect its neighbor.

One question regarding the interpretation of the above results concerns whether they apply to actively cycling bridges or to rigor-SLADP bridges. Several results suggest that at least a major fraction of the cross-bridges were actively cycling in both preparations. The rate of tension decrease upon addition of  $V_i$  is a measure of the fraction of active bridges, because addition of  $V_i$  to rigor-ADP bridges

does not cause a change in tension, nor does it lead to trapping of the nucleotide with  $V_i$  (23). The rates were similar for SLATP and for ATP, suggesting that a large fraction of the myosin heads were cycling, even in the absence of a regeneration system. The requirement for a regeneration system is mitigated by the fact that we used slow fibers, and that the hydrolysis rate for the SLATP is only 1/3 that of ATP. The fibers in the EPR cell are both generating tension, and are hydrolyzing the SLATP similarly to observed for single fibers. These results were all obtained in the absence of  $V_i$ . In the presence of a high concentration of  $V_i$  there will be potentially many fewer rigor-SLADP bridges, due to the decline of the hydrolysis rate in the fibers. It is important that this is exactly where our data are most meaningful, as discussed above. We conclude that our results were obtained for fibers that have a large fraction of active cross-bridges, particularly in the presence of high  $V_i$ , however the presence of some rigor-SLADP cross-bridges cannot be excluded. We also note that the actomyosin cycle in the presence of SLATP is different from that in the case of ATP, with a higher fraction of the myosin heads bound to actin. However the basic mechanism of force generation appears to be similar for the two nucleotides, so that if cooperative interactions played a major role in force generation it would be evident in both nucleotides.

We have shown that at very low levels of force (down to 1% of maximal) due to inhibition by high  $[V_i]$ , shortening velocity in fast fibers remains high at temperatures above 22°C (25). Structurally the heads trapped by  $V_i$  seem to stay close to the myosin rod, away from the thin filament (41), and fiber stiffness declines almost in proportion with force (42). These results account for this lack of internal drag. Since velocity remains high at these low force levels where only one head of any myosin molecule is functioning, a myosin molecule in a fast-twitch fiber under these conditions with one functional head promotes the same velocity of fiber shortening as either head of a myosin molecule with neither head trapped.

## CONCLUSION

The results obtained in this paper provide a rather definitive answer to the questions on head-head interactions discussed above. By eliminating myosin heads *via* the trapping of a myosin-MgADP- $V_i$  complex and measuring the fraction of myosin heads that have been trapped, we showed that elimination of one myosin head during maximal  $Ca^{2+}$ -activation has no effect on the ability of its neighboring head to generate isometric tension. Thus the results suggest that there are no cooperative interactions, either positive or negative, which modulate the ability of one myosin head to interact with actin during maximal  $Ca^{2+}$ -activation. Therefore, why does myosin have two heads? The myosin molecule might have two heads because it needs two tails (3). In other words, it needs a coiled-coil tail either for structural integrity of the myosin dimer or of the thick filaments, or because this is an efficient way to pack a maximal number of myosin heads into the defined space within the myofilament lattice (14).

We are grateful to Dr. E. Pate for helpful discussions and we would like to thank Mr. Michael Isard for modifications to the computer



software used to collect data from the tensiometer and the EPR spectrometer. Dr. Brett Hambly and Mrs. Kathy Franks-Skiba kindly provided the myosin species used.

## REFERENCES

1. Slayter, H.S. and Lowey, S. (1967) Substructure of the myosin molecule as visualized by electron microscopy. *Proc. Natl. Acad. Sci. USA* **58**, 1611-1618
2. Bagshaw, C.R. (1980) Divalent metal ion binding and subunit interactions in myosins: a critical review. *J. Muscle Res. Cell Motil.* **1**, 255-277
3. Bagshaw, C.R. (1987) Are two heads better than one? *Nature* **326**, 746-747
4. Kunz, P.A., Loth, K., Watterson, J.G., and Schaub, M.C. (1980) Nucleotide induced head-head interaction in myosin. *J. Muscle Res. Cell Motil.* **1**, 15-30
5. Chaen, S., Shimada, M., and Sugi, H. (1986) Evidence for cooperative interactions of myosin heads with thin filament in the force generation of vertebrate skeletal muscle fibers. *J. Biol. Chem.* **261**, 13632-13636
6. Geeves, M.A. (1991) The dynamics of actin and myosin association and the crossbridge model of muscle contraction. *Biochem. J.* **274**, 1-14
7. Wells, C. and Bagshaw, C.R. (1983) Segmental flexibility and head-head interaction in scallop myosin: a study using saturation transfer electron paramagnetic resonance spectroscopy. *J. Mol. Biol.* **164**, 137-157
8. Cremonesi, C.R., Sellers, J.R., and Facemyer, K.C. (1995) Two heads are required for phosphorylation-dependent regulation of smooth muscle myosin. *J. Biol. Chem.* **270**, 2171-2175
9. Spudich, J.A. and Watt, S. (1971) The regulation of rabbit skeletal muscle contraction. I. Biochemical studies of the interaction of the tropomyosin-troponin complex with actin and the proteolytic fragments of myosin. *J. Biol. Chem.* **246**, 4866-4871
10. Margossian, S.S. and Lowey, S. (1982) Preparation of myosin and its subfragments from rabbit skeletal muscle. *Methods Enzymol.* **85**, 55-71
11. Kodama, T., Fukui, K., and Kometani, K. (1986) The initial phosphate burst in ATP hydrolysis by myosin and subfragment-1 as studied by a modified Malachite Green method for determination of inorganic phosphate. *J. Biochem.* **99**, 1465-1472
12. Harada, Y., Noguchi, A., Kishino, A., and Yanagida, T. (1987) Sliding movement of single actin filaments on one-headed myosin filaments. *Nature* **326**, 805-808
13. Toyoshima, Y.Y., Kron, S.J., McNally, E.M., Niebling, K.R., Toyoshima, C., and Spudich, J.A. (1987) Myosin subfragment-1 is sufficient to move actin filaments *in vitro*. *Nature* **328**, 536-539
14. Cooke, R. and Franks, K.E. (1978) Generation of force by single-headed myosin. *J. Mol. Biol.* **120**, 361-373
15. Kishino, A. and Yanagida, T. (1988) Force measurements by micromanipulation of a single actin filament by glass needles. *Nature* **334**, 74-76
16. Molloy, J.E., Burns, J.E., Kendrick-Jones, J., Tregear, R.T., and White, D.C.S. (1995) Movement and force produced by a single myosin head. *Nature* **378**, 209-212
17. Kay, L.E., Pascone, J.M., Sykes, B.D., and Shriver, J.W. (1987) <sup>19</sup>F nuclear magnetic resonance as a probe of structural transitions and cooperative interactions in heavy meromyosin. *J. Biol. Chem.* **262**, 1984-1988
18. Huxley, A.F. (1957) Muscle structure and theories of contraction. *Prog. Biophys. Biophys. Chem.* **7**, 255-318
19. Goodno, C.C. (1982) Myosin active site trapping with vanadate ion. *Methods. Enzymol.* **85**, 116-123
20. Yount, R.G., Lawson, D., and Rayment, I. (1995) Is myosin a "back door" enzyme? *Biophys. J.* **68**, 44s-49s
21. Smith, C.A. and Rayment, I. (1996) X-ray structure of the magnesium(II)-ADP-vanadate complex of the *Dictyostelium discoideum* myosin motor domain to 1.9 Å resolution. *Biochemistry* **35**, 5404-5417
22. Wells, C. and Bagshaw, C.R. (1984) The characterization of vanadate-trapped nucleotide complexes with spin-labelled myosins. *J. Muscle Res. Cell Motil.* **5**, 97-112
23. Dantzig, J.A. and Goldman, Y.E. (1985) Suppression of muscle contraction by vanadate: mechanical and ligand binding studies on glycerol-extracted rabbit fibers. *J. Gen. Physiol.* **86**, 305-327
24. Crowder, M.S. and Cooke, R. (1987) Orientation of spin-labeled nucleotides bound to myosin in glycerinated muscle fibers. *Biophys. J.* **51**, 323-333
25. Pate, E., Wilson, G.J., Bhimani, M., and Cooke, R. (1994) Temperature dependence of the inhibitory effects of orthovanadate on shortening velocity in fast skeletal muscle. *Biophys. J.* **66**, 1554-1562
26. Wilson, G.J., Shull, S.E., and Cooke, R. (1995) Inhibition of muscle force by vanadate. *Biophys. J.* **68**, 216-226
27. Reedy, M.K., Lucaveche, C., Naber, N., and Cooke, R. (1992) Insect crossbridges, relaxed by spin-labeled nucleotide, show well-ordered 90° state by X-ray diffraction and electron microscopy, but spectra of electron paramagnetic resonance probes report disorder. *J. Mol. Biol.* **227**, 678-697
28. Wilson, G.J., dos Remedios, C.G., Stephenson, D.G., and Williams, D.A. (1991) Effects of sulphhydryl modification on skinned rat skeletal muscle fibres using 5,5'-dithiobis(2-nitrobenzoic acid). *J. Physiol.* **437**, 409-430
29. Pate, E.F. and Cooke, R. (1985) The inhibition of muscle contraction by adenosine 5'( $\beta,\gamma$ -imido) triphosphate and by pyrophosphate. *Biophys. J.* **47**, 773-780
30. Stephenson, D.G., Stewart, A.W., and Wilson, G.J. (1989) Dissociation of force from myofibrillar MgATPase and stiffness at short sarcomere lengths in rat and toad skeletal muscle. *J. Physiol.* **410**, 351-366
31. Weeds, A.G. and Taylor, R.S. (1975) Separation of myosin subfragment-1 isoenzymes from rabbit skeletal muscle myosin. *Nature* **257**, 54-56
32. Cooke, R. (1972) A new method for preparing myosin subfragment-1. *Biochem. Biophys. Res. Commun.* **49**, 1021-1028
33. Hambly, B., Franks, K., and Cooke, R. (1992) Paramagnetic probes attached to a light chain on the myosin head are highly disordered in active muscle fibers. *Biophys. J.* **63**, 1306-1313
34. Cooke, R., Crowder, M.S., and Thomas, D.D. (1982) *Nature* **300**, 776-778
35. Greene, L.E. and Eisenberg, E. (1980) The binding of heavy meromyosin to F-actin. *J. Biol. Chem.* **255**, 549-554
36. Fajer, P.G., Fajer, E.A., Brunsvold, N.J., and Thomas, D.D. (1988) Effects of AMPPNP on the orientation and rotational dynamics of spin-labeled muscle cross-bridges. *Biophys. J.* **53**, 513-524
37. Root, D.D., Cheung, P., and Reisler, E. (1991) Catalytic cooperativity induced by SH1 labeling of myosin filaments. *Biochemistry* **30**, 286-294
38. Reisler, E. (1982) Sulphydryl modification and labelling of myosin. *Methods Enzymol.* **85**, 84-93
39. Crowder, M.S. and Cooke, R. (1984) The effect of myosin sulphhydryl modification on the mechanics of fibre contraction. *J. Muscle Res. Cell Motil.* **5**, 131-146
40. Titus, M.A., Ashiba, G., and Szent-Gyorgyi, G.A. (1989) SH-1 modification of rabbit myosin interferes with calcium regulation. *J. Muscle Res. Cell Motil.* **10**, 25-33
41. Takemori, S., Yamaguchi, M., and Yagi, N. (1995) An X-ray diffraction study on a single frog skinned muscle fiber in the presence of vanadate. *J. Biochem.* **117**, 603-608
42. Chase, P.B., Martyn, D.A., Kushmerick, M.J., and Gordon, A.M. (1993) Effects of inorganic phosphate analogues on stiffness and unloaded shortening of skinned muscle fibres from rabbit. *J. Physiol.* **460**, 231-246